mathematics

MDPI

Article

Parity Deformed Tavis-Cummings Model: Entanglement, Parameter Estimation and Statistical Properties

Mariam Algarni [1], Kamal Berrada [2,3,*], Sayed Abdel-Khalek [4,5] and Hichem Eleuch [6,7,8]

[1] Department of Mathematical Sciences, College of Science, Princess Nourah Bint Abdulrahman University, P.O. Box 84428, Riyadh 11671, Saudi Arabia
[2] Department of Physics, College of Science, Imam Mohammad Ibn Saud Islamic University (IMSIU), P.O. Box 5701, Riyadh 11432, Saudi Arabia
[3] The Abdus Salam International Centre for Theoretical Physics, Strada Costiera 11, 34151 Trieste, Italy
[4] Department of Mathematics and Statistics, College of Science, Taif University, P.O. Box 11099, Taif 21944, Saudi Arabia
[5] Department of Mathematics, Faculty of Science, Sohag University, Sohag 82524, Egypt
[6] Department of Applied Physics and Astronomy, University of Sharjah, Sharjah 27272, United Arab Emirates
[7] College of Arts and Sciences, Abu Dhabi University, Abu Dhabi 59911, United Arab Emirates
[8] Institute for Quantum Science and Engineering, Texas A&M University, College Station, TX 77843, USA
* Correspondence: kaberrada@imamu.edu.sa

Abstract: In this paper, we introduce the parity extension of the harmonic oscillator systems to develop the generalized Tavis-Cummings model (T-CM) based on a specific deformation of the Heisenberg algebra. We present a quantum scheme of a two-qubit system (TQS) interacting with a quantized field that is initially prepared in parity deformed coherent states (PDCSs). The dynamical features of the considered system are explored in the presence of parity deformed parameter (PDP) and time-dependent coupling (t-dc). In particular, we examine the amount of the entanglement formed in the qubit–field and qubit–qubit states. We find that the maximal amount of the entanglement may be occurred periodically during the time evolution. Finally, we investigate the influence of PDP on the Fisher information and the photon statistics of the deformed field with respect to the main parameters of the system.

Keywords: two-qubit system; parity deformed coherent states; population; entanglement; fisher information; concurrence

MSC: 81V80

Citation: Algarni, M.; Berrada, K.; Abdel-Khalek, S.; Eleuch, H. Parity Deformed Tavis-Cummings Model: Entanglement, Parameter Estimation and Statistical Properties. *Mathematics* **2022**, *10*, 3051. https://doi.org/10.3390/math10173051

Academic Editor: Dmitry Makarov

Received: 9 July 2022
Accepted: 14 August 2022
Published: 24 August 2022

1. Introduction

Quantum entanglement (QE) is a kind of nonlocal correlation that is regarded as an essential concept in quantum mechanics theory, providing the features that distinguish quantum systems from their classical counterparts [1,2]. As a result of technological advances over the past few decades, QE has become the powerful resource and the core of various quantum technologies, including quantum metrology [3–5], quantum thermodynamics [6,7] and solid-state physics [8–12]. Therefore, the characterization and quantification of QE have attracted significant research interest [1,2,13]. Advances in quantum information technology have provided more information about the nonlocal correlation and increased awareness of it. Significant physical phenomena, such as QE sudden birth and QE sudden death, were investigated [14,15]. Therefore, the treatment and transmission of quantum information during the dynamics is limited by the decoherence effect. In such a situation, discussion of dynamical decay, studies and protection of stabilization of QE become of crucial significance.

In the past few decades, the concept of coherent states (CSs) has been incorporated into a large number of researches in the area of quantum optics and information. At the

beginning, Schrödinger presented CSs as non-propagating wave packet that minimize quantum mechanical uncertainty for systems with harmonic oscillator Hamiltonian [16]. These CSs exhibit the classical equations for the harmonic oscillator and that the expectation values of the momentum and coordinate operators oscillate in time in just in the same way as the case in the classical theory. Thereafter, Glauber showed that these states can be established by using the displacement operator on the ground state or as an eigenket of the annihilation operator [17]. In point of fact, the last two ideas led to the build of CSs in two distinct classes, the so-called Barut-Girardello and Klauder-Perelomov CSs [18,19]. Many generalizations with applications of these states have been considered in the literature [20–23]. Furthermore, by using the deformed Heisenberg algebra, the notion of the deformed harmonic oscillator was introduced and considered as a nonlinear oscillator with a particular kind of nonlinearity [24–28].

Recently, the concept of quantum Fisher information (QFI) has played a crucial role in the parameter estimation theory by characterizing the precision limits of quantum measurements [29]. It has significant applications in quantum technology, including the quantum frequency standards [30], clock synchronization [31] and measurement of gravity acceleration [32]. The QFI effectively characterizes the statistical distinguishability about a parameter that is encoded in a quantum state and delimits the parameter-estimation precision through the inequality so-called Cramer-Rao inequality [33–35], where the lower bound is provided by the QFI. It exhibits a specific bound for distinguishing the family members of probability distributions and shows the limit for which the quantum states are distinguished through measurements. It is crucial to take into account the connection between the concept of QFI and other key phenomena such as QE and squeezing. In this context, it was shown that the QFI can be used to comprehend the QE of multi-partite states [36,37]. Moreover, it was proven that the QE criterion provided through the QFI is stronger than that exhibited through spin squeezing phenomenon. On the subject of open systems and nonunitary evolutions, QFI is considered in the framework of finite systems to estimate the noise parameter of amplitude-damping [38,39] and depolarizing channels [40]. By using Gaussian squeezed probes, the estimation of the loss parameter can be improved in the presence of a bosonic channel [41]. Recently, researchers have utilized the parameter estimation problem in the quantum systems to explain the phase transitions [42,43].

The Jaynes-Cummings (J-CM) model has been widely utilized in quantum optics to describe the two-level atom–field interaction, where the applications and solvability of this model have long been discussed [44]. This model is utilized to describe several quantum phenomena, such as revival and collapse phenomena, atom–field entanglement and Rabi oscillations [45]. Recently the J-CM has been playing a major role in quantum information processing and considered one of the most important possible schemes for the production of non-classical states [46]. The quantum dynamics predictions of J-CM have been validated using a Rydberg atom in a QED cavity [45]. Since this model is an ideal in the framework of quantum optics, its extensions such as multi-photon transitions, cavity field with three- (or four)-level atoms and T-CM were considered [47–53]. On the other hand, the methods of algebraic operators have been used to study other extensions of J-CM. It is proven that the usual annihilation and creation and operators in the standard J-CM may be replaced by the deformed operators to form so-called deformed J-CM [54–56].

By considering the parity extension of the standard J-CM model, the aim of this work is to explore a quantum system that consists of a TQS interacting with a quantized field that is initially prepared in PDCSs. We investigate the dynamical features in the considered system in the absence and presence of PDP and t-dc effects. In particular, we examine the amount of the entanglement formed in the qubit–field and qubit–qubit states. Moreover, we consider the influence of PDP on the Fisher information and the photon statistics of the deformed field with respect to the main parameter of the system.

The remaining sections of the article are structured as follows. We provide a physical description of the quantum system and its dynamics in Section 2. The quantumness

quantifiers are presented in Section 3 together with the numerical results. In Section 4, we give our conclusions.

2. Physical Model

The Hamiltonian describing the interaction of each qubit, two-level atom, of the TQS with an upper (lower) state $|0_j\rangle$ ($|1_j\rangle$) with a one-mode field is given by

$$\hat{H}_I(t) = \sum_{k=1}^{2} D_k(t)\left(A|0_k\rangle\langle 1_k| + \mathrm{A}^+|1_k\rangle\langle 0_k|\right), \tag{1}$$

where A (A^+) represents the annihilation (creation) operator and $D_k(t)$ characterizes the t-dc strength between each qubit and the field. We consider the case of two identical qubits where $D_1(t) = D_2(t) = D(t)$ and $D(t) = s\ \sin(\mathrm{t})$. The t-dc is considered to be cosine or sine function. In this context, the coupling varies rapidly with time is of interest. New physical situations can be modeled through the generalization from the coupling D to arbitrary t-dc D(t). An implementation of particular interest is used when D(t) is the consideration of the time-dependent alignment of the atomic/molecular dipole moment using laser pulse [57] and motion of atoms inside the cavity. Recently, a study of a cavity-QED system adjusted by employing bichromatic adiabatic passage in the presence of dissipation [58], where this study examined the generation of a controlled Fock state through the cavity by considering a traveling atomic system that encounters t-dc.

Here, we introduce the parity Heisenberg algebra (PHA) for considering the parity extension of the quantum model described by the Hamiltonian (1). This algebra is defined through by the operators $\{I, A, \mathrm{A}^+, \mathrm{P}\}$ that obey the following commutation and anti-commutation relations

$$\left[A, A^+\right] = 1 + 2\lambda P,\ \left\{P, A^+\right\} = \{P, A\} = 0. \tag{2}$$

Here, I and R are the identity and parity operators, respectively, and λ represents a deformed parameter. The operator P satisfies

$$P^+ = P^{-1} = P,\ P^2 = I, \tag{3}$$

acting on the Fock state as

$$P|n\rangle = (-1)^n|n\rangle. \tag{4}$$

The number operator N, $N|n\rangle = n|n\rangle$, is quite different from the operator A^+A and it verifies

$$A^+A = N + \lambda(1 - P), \qquad \left[N, A^+\right] = A^+, \qquad [N, A] = -A. \tag{5}$$

with the following irreducible representation

$$A|2n\rangle = (2n)^{\frac{1}{2}}|2n-1\rangle, \qquad A^+|2n\rangle = (2n + 2\lambda + 1)^{\frac{1}{2}}|2n+1\rangle \tag{6}$$

$$A|2n+1\rangle = (2n + 2\lambda + 1)^{\frac{1}{2}}|2n+1\rangle, \quad A^+|2n+1\rangle = (2n+2)^{\frac{1}{2}}|2n+2\rangle. \tag{7}$$

The operators A and A^+ are related to the usual operators a and a^+ as follows [56]:

$$A = a - \frac{\lambda}{\sqrt{2}\,x}P,\ A^+ = a^+ + \frac{\lambda}{\sqrt{2}x}P. \tag{8}$$

In the limit $\lambda \to 0$, we find that the ordinary case, $[A, A^+] \to [\mathrm{a}, \mathrm{a}^+] = 1$, is recovered and the model described by the Hamiltonian (1) represents the standard T-CM.

The coherent states, PDCSs, associated with the parity field are introduced as an eigenket of the square of the annihilation operator, $\hat{A}^2|\alpha\rangle_\lambda = \alpha^2|\alpha\rangle$. The PDCSs is given by [56]

$$|\Psi_F(0)\rangle = \sqrt{\frac{\alpha^{2\lambda-1}}{2^{\lambda-1/2}I_{\lambda-1/2}}}\sum_{m=0}^{\infty}\left(\frac{\alpha^{2m}}{2^n\sqrt{\Gamma(m+1)\Gamma(m+\lambda+1/2)}}\right)|2m\rangle. \tag{9}$$

These states exhibit properties like the Wigner negative binomial states.
The TQS−Field state at subsequent time can be formulated as

$$\begin{aligned}|\Psi_{TQS-F}(st)\rangle = \sum_{m=0}^{\infty}(&R_1(m,st)|2m,0_10_2\rangle + R_2(m,st)|2m+1,0_11_2\rangle\\ &+R_3(m,st)|2m+1,1_10_2\rangle + R_4(m,st)|2m+2,1_11_2\rangle).\end{aligned} \tag{10}$$

The coefficients R_{i} can be obtained through solving the Schrödinger equation

$$i\,\hbar\,\frac{\partial}{\partial t}\,|\Psi_{\mathrm{TQS-F}}(t)\rangle = \hat{H}_I(t)\big|\Psi_{TQS-F}(0)\big\rangle. \tag{11}$$

The initial quantum state of the whole system is considered to be

$$\begin{aligned}\big|\Psi_{TQs-F}(0)\big\rangle &= |\Psi_{\mathrm{TQS}}(0)\rangle\otimes|\Psi_F(0)\rangle\\ &= (\cos(\theta)|0_10_2\rangle + \sin(\theta)|1_11_2\rangle)\otimes\sum_{m=0}^{\infty}\mathrm{Q}_m|2m\rangle,\end{aligned} \tag{12}$$

where the amplitude Q_m is defined by Equation (9). For $\theta = 0$, the TQS initially is in the separable state and for $\theta = \pi/4$, and the TQS initially is in the Bell state.

Substituting Equation (10) into (11) and using the initial condition (12), the coefficients R_{i} are given as

$$\begin{aligned}R_1(2m,st) = \tfrac{Q_m(\lambda)}{4m+2\lambda+3}&[cos\theta\{2m+2+(2m+2\lambda+1)cos(d(t)\xi_m(\lambda))\}\\ &+\sqrt{(2m+2\lambda+1)(2m+2)}sin\theta\{cos(d(st)\xi_m(\lambda))-1\}],\end{aligned} \tag{13}$$

$$\begin{aligned}R_2(2m,st) &= R_3(2m,st)\\ &= \tfrac{-iQ_m(\lambda)sin(d(st)\xi_m(\lambda))}{\xi_m(\lambda)}[cos\theta\sqrt{2m+2\lambda+1}\\ &\quad +sin\theta\sqrt{2m+2}],\end{aligned} \tag{14}$$

$$\begin{aligned}R_4(2m,st) = \tfrac{Q_m(\lambda)}{4m+2\lambda+3}&\Big[\sqrt{(2m+2\lambda+1)(2m+2)}cos\theta\{cos(d(st)\xi_m(\lambda))\\ &-1\}+sin\theta\{(2m+2)cos(d(t)\xi_m(\lambda))+2m+2\lambda+1\}],\end{aligned} \tag{15}$$

where

$$\xi_m(\lambda) = \sqrt{8m+4\lambda+6}. \tag{16}$$

From the total density matrix $\rho_{TQS-F}(st) = \big|\Psi_{TQS-F}(st)\rangle\langle\Psi_{TQS-F}(st)\big|$, the reduced density matrix of the TQS (field) contributed by $\rho_F(st)\big(\rho_{TQS}(st)\big)$ is obtained as

$$\rho_{\mathrm{TQS}}(st) = Tr_F\{\rho_{\mathrm{TQS-F}}(st)\} = \sum_{j=1}^{4}\sum_{n=1}^{4}\rho_{jn}|j\rangle\langle n|, \tag{17}$$

$$\rho_{\mathrm{F}}(st) = Tr_{TQS}\{\rho_{\mathrm{TQS-F}}(st)\} = \sum_{k}^{\infty}\rho_k|k\rangle\langle k|. \tag{18}$$

The QE and FI of the TQS state will be obtained through the time variation of the elements of the matrix defined in Equation (17). The photon statistics of the radiation field

can be studied via the evolution of the Mandel parameter based on the evolution of the field density matrix given by Equation (18).

3. Quantum Measures and Numerical Results

Here, we define the different measures of quantumness and discuss their behavior with respect to t-dc and PDP effects.

3.1. Atomic Inversion

The population inversion is defined as the difference between the excited and ground state populations. The atomic population inversion of the TQS can be written by

$$\rho_z(t) = \sum_{m=0}^{\infty} \left(R_1(m,st)^2 + R_2(m,st)^2 - R_3(m,st)^2 - R_4(m,st)^2 \right) \tag{19}$$

In Figure 1, we illustrate the evolution of the population inversion, ρ_z, of TQS with $\lambda = 0$ and $\lambda = 50$. Generally, it is obvious that the dynamical behavior of the function ρ_z is influenced by the parameters λ and D. In the absence of t-dc and PDP effects, we find that the function ρ_z exhibits fast oscillations with collapse and revival phenomena. The collapse period occurs for small intervals of time and the amplitude of the function ρ_z decreases with time. In the existence of the t-dc effect, the oscillations of function ρ_z become regular, exhibiting a periodic behavior. Moreover, we notice that the period of the collapse remains constant during the dynamics. On the other hand, the presence PDP effect leads to raise the amplitude of oscillations of the atomic inversion accompanied with the collapse phenomenon in the absence of t-dc effect during the time evolution. From this result, we can conclude that the nonlinearity of field will enhance the amplitude of oscillations in the population of the TQS with the revival and collapse phenomena and that the existence of the t-dc will result the periodic behavior of ρ_z during the dynamics.

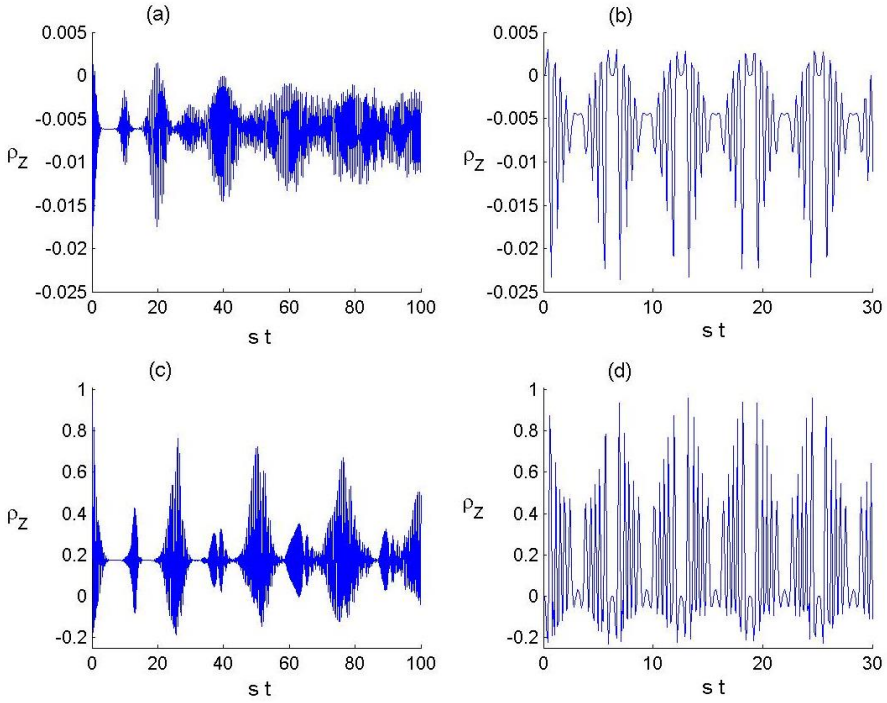

Figure 1. Time variation of the atomic population inversion ρ_z for the TQS with $\theta = \pi/4$ and the radiation field in the PDCSs. Panels (**a**,**b**) correspond to the case of absence of the PDP effect (i.e., $\lambda = 0$) for constant $(D(\mathrm{t}) = \mathrm{s})$ and t-dc $(D(\mathrm{t}) = \mathrm{s}\ \sin(\mathrm{t}))$, respectively. Panels (**c**,**d**) are, respectively, the same as (**a**,**b**) but in the presence of the PDP effect with $\lambda = 50$.

3.2. Qubits–Field Entanglement

The results of the quantum entanglement evolution of the qubits–field state using the subsystem systemare obtained by using the von-Neumann entropy as

$$E_{\mathrm{F-TQS}} = -\mathrm{Tr}\{\rho_{\mathrm{TQS}} \ln[\rho_{\mathrm{TQS}}]\}. \tag{20}$$

Here, ρ_{TQS} represents the TQS density operator given by Equation (17). The function $E_{\mathrm{F-TQS}}$ takes the form

$$E_{\mathrm{F-TQS}} = -\sum_{\mathrm{i}} \varpi_{\mathrm{i}} \ln \varpi_{\mathrm{i}}, \tag{21}$$

where ϖ_{i} are the eigenvalues of the state ρ_{TQS}.

In Figure 2, we plot the dynamical behavior of the von Neumann entropy according to the parameter values of the physical model. We consider the four physical situations that depend on λ and D. Figure 2a–d displays the dynamical behaviour of the quantum entropy according the same condition of the physical parameters as above. In the $\lambda \to 0$ limit and $D(\mathrm{t}) = \mathrm{s}$, we can observe that the $E_{\mathrm{F-TQS}}$ function increases with time and presents an oscillatory behavior with a steady comportment of oscillations for large times. In the $t \to \infty$ limit, the TQS is trapped by the parity field and that the QE of the TQS–field state stabilizes at a certain range of time values, exhibiting the same behavior of the population inversion. In the $\lambda \to 0$ limit and $D(\mathrm{t}) = s\, sin(t)$, the $E_{\mathrm{F-TQS}}$ function oscillates with time as a periodic function with the same time period of oscillations of the population inversion. Furthermore, the maximum value of QE is diminished during the dynamics in comparison with the case of $D(\mathrm{t}) = \mathrm{s}$. For $\lambda \to 50$, we find that the behavior of the $E_{\mathrm{F-TQS}}$ function is not strongly changed with time and that the TQS–field state reaches the maximum value of entanglement in the existence of t-dc effect. We can conclude that the amount of the entanglement is more sensitive to the t-dc in comparison to the nonlinearity of the field.

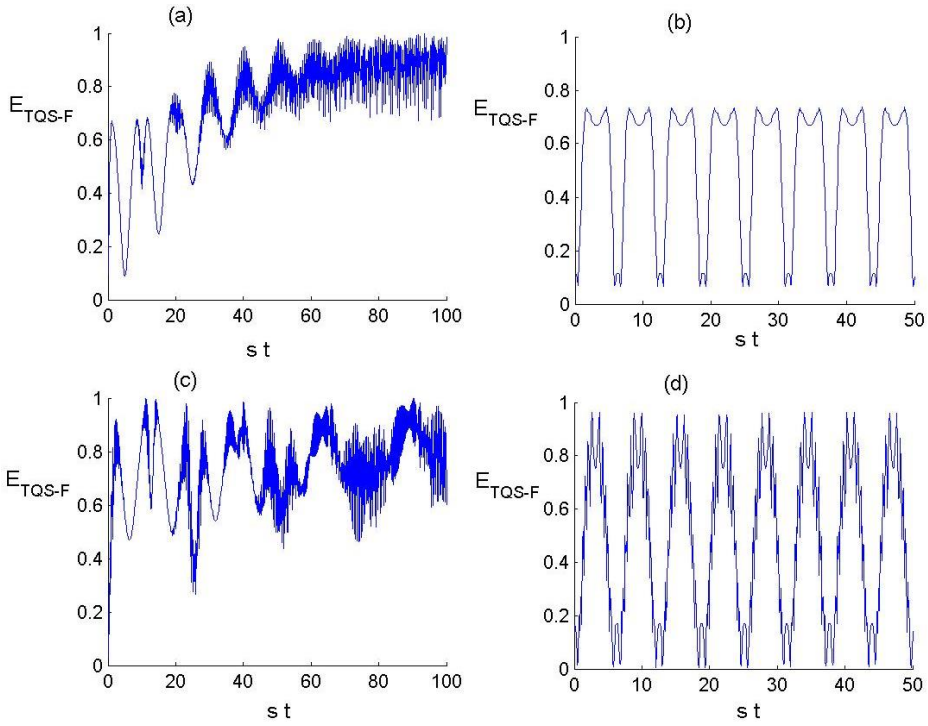

Figure 2. Time evolution of the QE of the TQS–field state denoted by $E_{\mathrm{TQS-F}}$. Panels (**a**,**b**) correspond to the case of absence of the PDP effect (i.e., $\lambda = 0$) for constant $(D(\mathrm{t}) = \mathrm{s})$ and t-dc $(D(\mathrm{t}) = \mathrm{s}\ \sin(\mathrm{t}))$, respectively. Panels (**c**,**d**) are, respectively, the same as (**a**,**b**) but in the presence of the PDP effect with $\lambda = 50$.

3.3. Qubit–Qubit Entanglement

We use the concurrence to measure the nonlocal correlation between the two qubits [59]. It is defined as

$$C_{12} : max\{0, \mu_1 - \mu_2 - \mu_3 - \mu_4\}\,, \tag{22}$$

where μ_j defines the eigenvalues given in decreasing order of the matrix $\rho_{\mathrm{TQS}}\widetilde{\rho}_{\mathrm{TQS}}$, where $\widetilde{\rho}_{\mathrm{TQS}}$ is the density matrix related to the Pauli matrix σ_Y and ρ^*_{TQS} (complex conjugate of ρ_{TQS}) by

$$\widetilde{\rho}_{\mathrm{TQS}} = (\sigma_Y \otimes \sigma_Y)\rho^*_{\mathrm{TQS}}(\sigma_Y \otimes \sigma_Y). \tag{23}$$

The state of TQS is in a separable state for $C_{12} = 0$, while the maximally entangled state is obtained for $C_{12} = 1$.

The dynamics of the concurrence with respect to the values of the different parameters of the system is displayed in Figure 3. Generally, it is clear that the dynamical behavior of the function C_{12} is very sensitive to values of λ and D. The value of concurrence ranges between 1 and 0, showing that the entanglement of the TQS state can be strong in some periods and weak in other ones contingent on the values of λ and D. In the absence of t-dc and PDP effects, we can observe that the function C_{12} starts from its maximal value 1, exhibits random oscillations and decreases with time until attain a steady behavior of random oscillations. Interestingly, the function C_{12} takes suddenly zero values for a finite time interval during the dynamics displaying sudden death and birth phenomena of entanglement. Moreover, we also observe that the periods of sudden phenomenon change during the dynamics. In the presence of the t-dc effect, the oscillations of concurrence become regular, exhibiting a periodic behavior during the dynamics and that the periods of the sudden death phenomenon remain constant during the dynamics. On the other hand, the PDP effects do not largely influence the behavior of the concurrence in the presence of t-dc effect. The presence of PDP and t-dc effects leads to decrease the maximal value of the concurrence as well as the time periods of the sudden death phenomenon. This result indicates that control and preservation of the entanglement of TQS state strongly depends on the interaction between the TQS and the parity field and that the dependence on the nonlinearity of the radiation field is stronger in the absence of the t-dc effect.

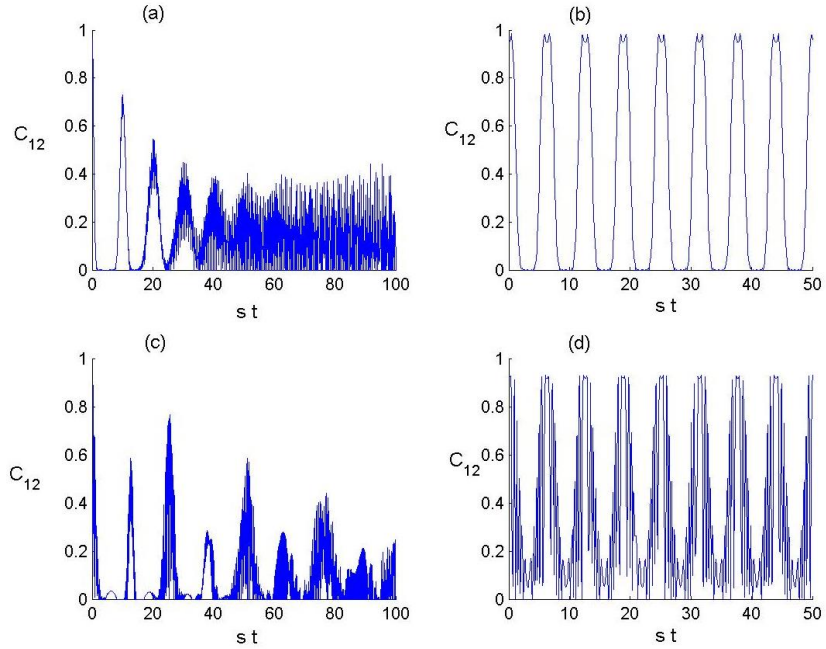

Figure 3. Time evolution of the TQS entanglement denoted by C_{12}. Panels (**a**,**b**) correspond to the case of absence of the PDP effect (i.e., $\lambda = 0$) for constant $(D(\mathrm{t}) = \mathrm{s})$ and t-dc $(D(\mathrm{t}) = \mathrm{s}\ \sin(\mathrm{t}))$, respectively. Panels (**c**,**d**) are, respectively, the same as (**a**,**b**) but in the presence of the PDP effect with $\lambda = 50$.

In Figure 4, we illustrate the time variation of the concurrence of TQS when the qubits are initially defined in a separate state. We can observe that it is possible to create entanglement using the model. That is to say, if starting with a fully separable state, it is possible to obtain an entangled state.

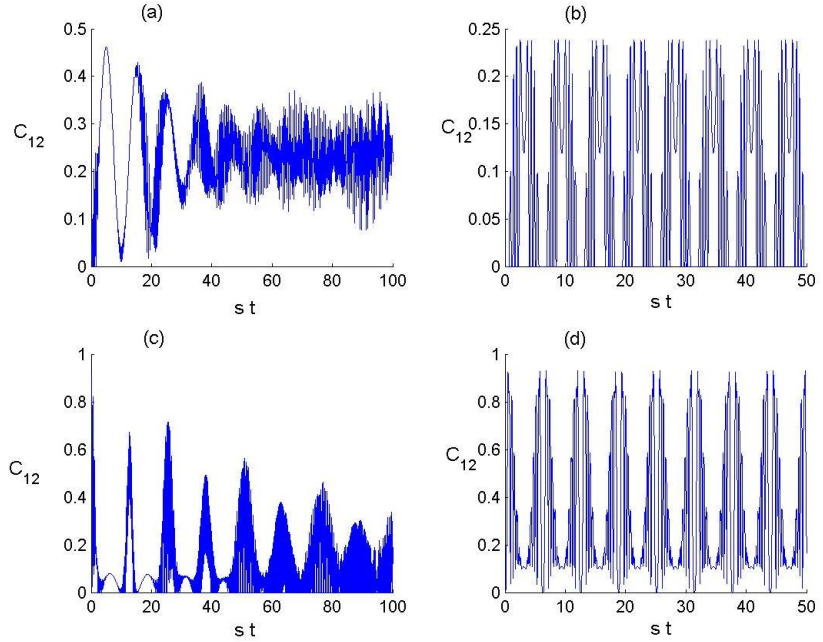

Figure 4. Time evolution of the TQS entanglement denoted by C_{12} when the TQS state is initially defined in a fully separable state, $\theta = 0$. Panels (**a**,**b**) correspond to the case of absence of the PDP effect (i.e., $\lambda = 0$) for constant $(D(\mathrm{t}) = \mathrm{s})$ and t-dc $(D(\mathrm{t}) = \mathrm{s}\ \sin(\mathrm{t}))$, respectively. Panels (**c**,**d**) are, respectively, the same as (**a**,**b**) but in the presence of the PDP effect with $\lambda = 50$.

3.4. Quantum Fisher Information

The QFI of TQS relies on the estimator parameter β, which is motivated by the shift parameter according to $W_{\hat{\vartheta}} = \frac{1}{\sqrt{2}}[exp(i\beta)|0_1 0_2\rangle + |1_1 1_2\rangle]$. Thus, the optimal target state is $W_{\hat{\vartheta}}|U(0)\rangle$ is

$$|U(0)\rangle_{opt} = \frac{1}{\sqrt{2}}\left[exp\ (i\beta)\ \frac{1}{\sqrt{2}}(|0_1 0_2\rangle + |1_1 1_2\rangle)\right] \otimes |U_F(0)\rangle\,. \tag{24}$$

The QFI is formulated as [25]

$$F_{\mathrm{TQS}}(st) = tr\{\rho_{\mathrm{TQS}}(\beta, st)L(\beta, st)^2\}, \tag{25}$$

where the TQS operator, ρ_{TQS}, is related to the symmetric logarithmic derivative operator $L(\beta, T)$ via the equation,

$$2\frac{\partial L(\beta, st)}{\partial t} = \rho_{\mathrm{TQS}}(\beta, st)L(\beta, T) + \mathrm{L}(\beta, T)\rho_{\mathrm{TQS}}(\beta, st). \tag{26}$$

In Figure 5, we depict the evolution of QFI versus the time st with respect to the values of the different parameters of the physical model. Generally, we can note that the enhancement and preservation of the parameter estimation precision strongly depends on the values of λ and D. From the figure, we can observe that the function F_{TQS} is affected in similar as the concurrence according to the values of λ and D, where the function F_{TQS} oscillates chaotically between the values 0 and 1 in the case of $D(\mathrm{t}) = s$, and its behavior becomes regular as a periodic function when $D(\mathrm{t}) = s\ sin(t)$ and attains the minimum and maximum values periodically, showing the flow change of the information between the

field and TQS. Furthermore, the presence of PDP leads to a raise in the value of minima of the function F_{TQS} and then enhances the precision of the parameter estimation during the dynamics.

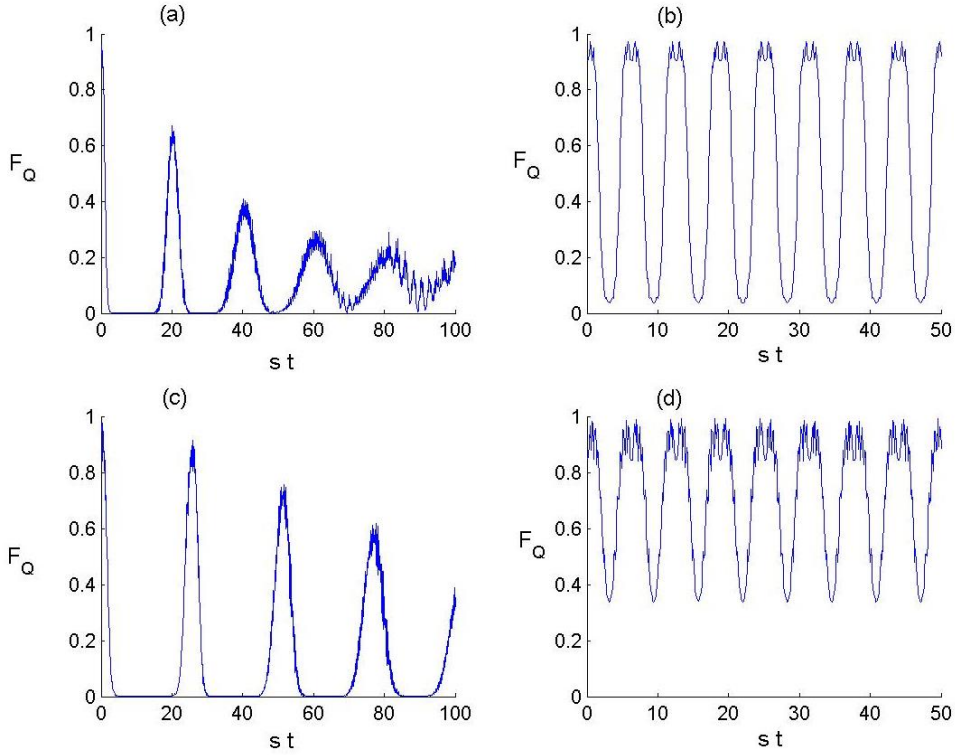

Figure 5. Time evolution of the QFI denoted by F_{TQS}. Panels (**a**,**b**) correspond to the case of absence of the PDP effect (i.e., $\lambda = 0$) for constant $(D(\mathrm{t}) = \mathrm{s})$ and t-dc $(D(\mathrm{t}) = \mathrm{s}\ \sin(\mathrm{t}))$, respectively. Panels (**c**,**d**) are, respectively, the same as (**a**,**b**) but in the presence of the PDP effect with $\lambda = 50$.

3.5. Field Photon Statistics

We introduce the Mandel parameter to examine the photons distribution in of the parity field. This parameter is defined as [60]

$$Q_M = \frac{Tr\left(\hat{A}^{\dagger}\hat{A}\right)^2}{Tr\left(\mathrm{A}^{\dagger}\hat{A}\right)} - Tr\left(\mathrm{A}^{\dagger}\hat{A}\right) - 1, \tag{27}$$

The field is governed by super-Poissonian statistics for $Q_M > 0$, Poissonian statistics for $Q_M = 0$ and sub-Poissonian statistics for $Q_M < 0$, which indicate that photons are antibunched. The sub-Poissonian statistics indicate that the field has a quantum nature.

In Figure 6, we display the dynamical behavior of the Mandel parameter to show the time variation of the statistical property of the deformed field according to the values of λ and D. Generally, it is clear that the time variation of the parameter Q_M is influenced by λ and D. In the $\lambda \to 0$ limit, we can observe that the parameter Q_M takes negative values exhibiting super-Poissonian behavior for both cases $D(\mathrm{t}) = \mathrm{s}$ and $D(\mathrm{t}) = s\ sin(t)$. On the other side, the statistics of the quantized field provides, in general, a super-Poissonian behavior for $\lambda > 0$.

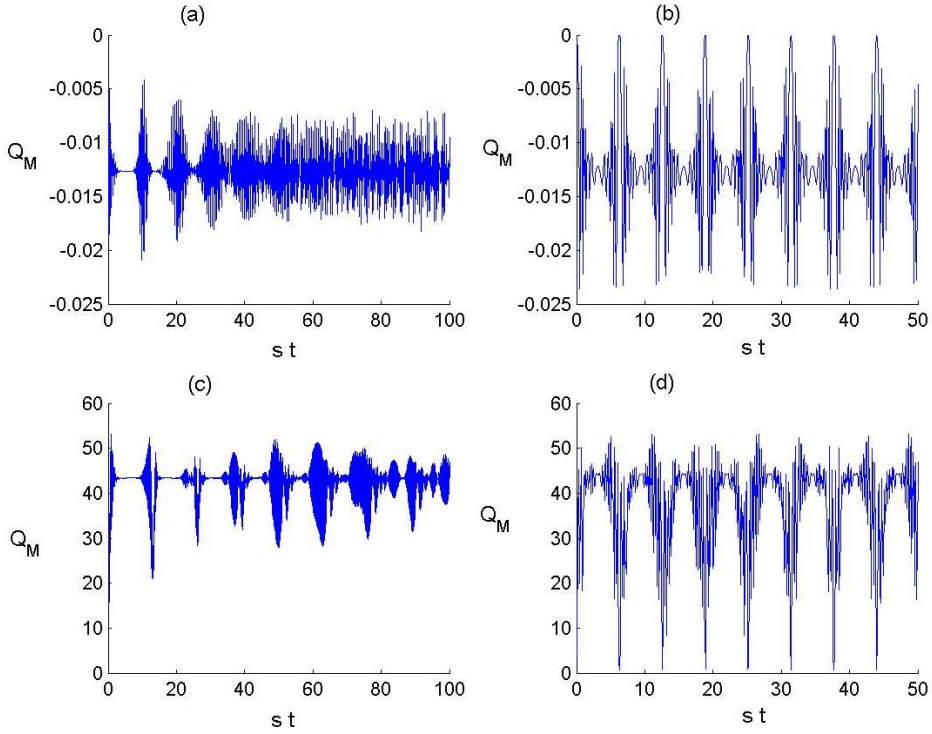

Figure 6. The time evolution of the Mandel parameter denoted by Q_M. Panels (**a**,**b**) correspond to the case of absence of the PDP effect (i.e., $\lambda = 0$) for constant $(D(\mathrm{t}) = \mathrm{s})$ and t-dc $(D(\mathrm{t}) = \mathrm{s}\ \sin(\mathrm{t}))$, respectively. Panels (**c**,**d**) are, respectively, the same as (**a**,**b**) but in the presence of the PDP effect with $\lambda = 50$.

4. Conclusions

In summary, we introduced the parity extension of the harmonic oscillator systems to develop the generalized T-CM based on a specific deformation of the Heisenberg algebra. We studied a system where a TQS is interacting with a quantized field that is initially prepared in the PDCSs. The dynamical features of the considered system were explored according the main physical parameters of the model. Generally, the PDP and t-dc effects were found very prominent on the dynamical properties of the quantumness measures. In particular, we examined the amount of the entanglement formed in the qubit–field and qubit–qubit states. The nonlocal correlation between the TQS and radiation field was provided by the evolution of von Neumann entropy. Whereas the concurrence was used to detect the qubit–qubit entanglement during the dynamics. We found that the maximal amount of the entanglement may have occurred periodically in the presence of t-dc effect. Moreover, we investigated the influence of PDP on the parameter estimation and the photon statistics of the deformed field according to the main parameters with and without the t-dc effect.

Author Contributions: M.A.: Visualization, supervision, project administration, reviewing and editing. K.B.: Conceptualization, methodology, writing—original draft, writing—reviewing and editing. S.A.-K.: Conceptualization, methodology, writing—original draft, writing—reviewing and editing. H.E.: Validation, funding acquisition, investigation. All authors have read and agreed to the published version of the manuscript.

Funding: Princess Nourah bint Abdulrahman University Researchers Supporting Project number (PNURSP2022R225), Princess Nourah bint Abdulrahman University, Riyadh, Saudi Arabia.

Institutional Review Board Statement: Not applicable.

Informed Consent Statement: Not applicable.

Data Availability Statement: Not applicable.

Conflicts of Interest: The authors declare no conflict of interest.

References

1. Nielsen, M.A.; Chuang, I.L. *Quantum Computation and Information*; Cambridge University Press: Cambridge, UK, 2000.
2. Alber, G.; Beth, T.; Horodecki, M.; Horodecki, P.; Horodecki, R.; Rotteler, M.; Weinfurter, H.; Zeilinger, R.A. *Quantum Information*; Springer: Berlin, Germany, 2001; Chapter 5.
3. Joo, J.; Munro, W.J.; Spiller, T.P. Quantum metrology with entangled coherent states. *Phys. Rev. Lett.* **2011**, *107*, 083601. [CrossRef] [PubMed]
4. Berrada, K.; Abdel-Khalek, S.; Raymond Ooi, C.H. Quantum metrology with entangled spin-coherent states of two modes. *Phys. Rev. A* **2012**, *86*, 033823. [CrossRef]
5. Berrada, K. Quantum metrology with SU (1, 1) coherent states in the presence of nonlinear phase shifts. *Phys. Rev. A* **2013**, *88*, 013817. [CrossRef]
6. Goold, J.; Huber, M.; Riera, A.; del Rio, L.; Skrzypczyk, P. The role of quantum information in thermodynamics—A topical review. *J. Phys. A Math. Theor.* **2016**, *49*, 143001. [CrossRef]
7. Kibe, T.; Mukhopadhyay, A.; Roy, P. Quantum Thermodynamics of Holographic Quenches and Bounds on the Growth of Entanglement from the Quantum Null Energy Condition. *Phys. Rev. Lett.* **2022**, *128*, 191602. [CrossRef]
8. Liu, C.; Tu, T.; Li, P.-Y.; Liu, X.; Zhu, X.-Y.; Zhou, Z.-Q.; Li, C.-F.; Guo, G.-C. Towards entanglement distillation between atomic ensembles using high-fidelity spin operations. *Commun. Phys.* **2022**, *5*, 67. [CrossRef]
9. Castelano, L.K.; Fanchini, F.F.; Berrada, K. Open quantum system description of singlet-triplet qubits in quantum dots. *Phys. Rev. B* **2016**, *94*, 235433. [CrossRef]
10. Pfaff, W.; Taminiau, T.H.; Robledo, L.; Bernien, H.; Markham, M.; Twitchen, D.J.; Hanson, R. Demonstration of entanglement-by-measurement of solid-state qubits. *Nat. Phys.* **2013**, *9*, 29. [CrossRef]
11. Aldaghfag, S.A.; Berrada, K.; Abdel-Khalek, S. Entanglement and photon statistics of two dipole–dipole coupled superconducting qubits with Kerr-like nonlineariti e. *Results Phys.* **2020**, *16*, 102978. [CrossRef]
12. Abdel-Khalek, S.; Berrada, K.; Aldaghfag, S.A. Quantum correlations and non-classical properties for two superconducting qubits interacting with a quantized field in the context of deformed Heisenberg algebra. *Chaos Solitons Fractals* **2021**, *143*, 110466. [CrossRef]
13. Horodecki, R.; Horodecki, P.; Horodecki, M.; Horodecki, K. Quantum entanglement. *Rev. Mod. Phys.* **2009**, *81*, 865. [CrossRef]
14. Eberly, J.H.; Yu, T. The end of an entanglement. *Science* **2007**, *316*, 555. [CrossRef] [PubMed]
15. Yu, T.; Eberly, J.H. Finite-time disentanglement via spontaneous emission. *Phys. Rev. Lett.* **2006**, *97*, 140403. [CrossRef]
16. Shrödinger, E. Der stetige Übergang von der Mikro-zur Makromechanik. *Naturwissenschafter* **1926**, *14*, 664. [CrossRef]
17. Glauber, R.J. Coherent and incoherent states of the radiation field. *Phys. Rev.* **1963**, *131*, 2766–2788. [CrossRef]
18. Perelomov, A.M. *Generalized Coherent States and Their Applications*; Springer: Berlin, Germany, 1986.
19. Ali, S.T.; Antoine, J.P.; Gazeau, J.P. *Coherent States, Wavelets and Their Generalizations*; Springer: Berlin, Germany, 2000.
20. Dodonov, V.V.; Malkin, I.A.; Man'ko, V.I. Even and odd coherent states and excitations of a singular oscillator. *Physica* **1974**, *72*, 597. [CrossRef]
21. Castaños, O.; López-Peña, R.; Man'ko, V.I.J. Crystallized Schrödinger cat states. *Russ. Laser Res.* **1995**, *16*, 477. [CrossRef]
22. Castaños, O.; López-Saldívar, J.A. Dynamics of Schrödinger cat states. *J. Phys. Conf. Ser.* **2012**, *380*, 012017. [CrossRef]
23. López-Saldívar, J.A. General superposition states associated to the rotational and inversion symmetries in the phase space. *Phys. Scr.* **2020**, *95*, 065206. [CrossRef]
24. Man'ko, V.I.; Marmo, G.; Sudarshan, E.C.G.; Zaccaria, F. f -Oscillators and nonlinear coherent states. *Phys. Scr.* **1997**, *55*, 528. [CrossRef]
25. Berrada, K.; Eleuch, H. Noncommutative deformed cat states under decoherence. *Phys. Rev. D* **2019**, *100*, 016020. [CrossRef]
26. Berrada, K.; Abdel-Khalek, S.; Raymond Ooi, C.H. Geometric phase and entanglement for a single qubit interacting with deformed-states superposition. *Quantum Inform. Process.* **2013**, *12*, 2177. [CrossRef]
27. Berrada, K.; Baz, M.E.; Hassouni, Y. Generalized spin coherent states: Construction and some physical properties. *J. Stat. Phys.* **2011**, *142*, 510. [CrossRef]
28. Berrada, K.; Baz, M.E. On the construction of generalized su (1, 1) coherent states. *Hassouni Rep. Math. Phys.* **2011**, *68*, 23. [CrossRef]
29. Fisher, R.A. Theory of statistical estimation. *Math. Proc. Camb. Philos. Soc.* **1925**, *22*, 700. [CrossRef]
30. Huelga, S.F.; Macchiavello, C.; Pellizzari, T.; Ekert, A.K.; Plenio, M.B.; Cirac, J.I. Improvement of frequency standards with quantum entanglement. *Phys. Rev. Lett.* **1997**, *79*, 3865. [CrossRef]
31. Jozsa, R.; Abrams, D.S.; Dowling, J.P.; Williams, C.P. Quantum clock synchronization based on shared prior entanglement. *Phys. Rev. Lett.* **2000**, *85*, 2010. [CrossRef]
32. Peters, A.; Chung, K.Y.; Chu, S. Measurement of gravitational acceleration by dropping atoms. *Nature* **1999**, *400*, 849. [CrossRef]
33. Helstrom, C.W. *Quantum Detection and Estimation Theory*; Academic Press, Inc.: New York, NY, USA, 1976.
34. Braunstein, S.L.; Caves, C.M. Statistical distance and the geometry of quantum states. *Phys. Rev. Lett.* **1994**, *72*, 3439. [CrossRef]
35. Braunstein, S.L.; Caves, C.M.; Milburn, G.J. Generalized uncertainty relations: Theory, examples, and Lorentz invariance. *Ann. Phys.* **1996**, *247*, 135. [CrossRef]

36. Boixo, S.; Monras, A. Operational interpretation for global multipartite entanglement. *Phys. Rev. Lett.* **2008**, *100*, 100503. [CrossRef] [PubMed]
37. Pezze, L.; Smerzi, A. Entanglement, nonlinear dynamics, and the Heisenberg limit. *Phys. Rev. Lett.* **2009**, *102*, 100401. [CrossRef] [PubMed]
38. Berrada, K. Non-Markovian effect on the precision of parameter estimation. *Phys. Rev. A* **2013**, *88*, 035806. [CrossRef]
39. Ji, Z.; Wang, G.; Duan, R.; Feng, Y. Parameter estimation of quantum channels. *IEEE Trans. Inf. Theory* **2008**, *54*, 5172. [CrossRef]
40. Fujiwara, A. Quantum channel identification problem. *Phys. Rev. A* **2001**, *63*, 042304. [CrossRef]
41. Monras, A.; Paris, M.G.A. Optimal quantum estimation of loss in bosonic channels. *Phys. Rev. Lett.* **2007**, *98*, 160401. [CrossRef]
42. Invernizzi, C.; Korbman, M.; Venuti, L.C.; Paris, M.G.A. Optimal quantum estimation in spin systems at criticality. *Phys. Rev. A* **2008**, *78*, 042106. [CrossRef]
43. Ma, J.; Wang, X. Fisher information and spin squeezing in the Lipkin-Meshkov-Glick model. *Phys. Rev. A* **2009**, *80*, 012318. [CrossRef]
44. Jaynes, E.; Cummings, F. Comparison of quantum and semiclassical radiation theories with application to the beam maser. *Proc. IEEE* **1963**, *51*, 89. [CrossRef]
45. Scully, M.O.; Zubairy, M.S. *Quantum Optics*; Cambridge University Press: Cambridge, UK, 2001.
46. Short, R.; Mandel, L. Observation of Sub-Poissonian Photon Statistics. *Phys. Rev. Lett.* **1983**, *51*, 384. [CrossRef]
47. Singh, S. Field statistics in some generalized Jaynes-Cummings models. *Phys. Rev. A* **1982**, *25*, 3206. [CrossRef]
48. Tavis, M.; Cummings, F.W. Exact solution for an N-molecule—radiation-field Hamiltonian. *Phys. Rev.* **1968**, *170*, 379. [CrossRef]
49. Tessier, T.E.; Deutsch, I.H.; Delgado, A.; Fuentes-Guridi, I. Entanglement sharing in the two-atom Tavis-Cummings model. *Phys. Rev. A* **2003**, *68*, 062316. [CrossRef]
50. López, C.E.; Lastra, F.; Romero, G.; Retamal, J.C. Entanglement properties in the inhomogeneous Tavis-Cummings model. *Phys. Rev. A* **2007**, *75*, 022107. [CrossRef]
51. Guo, J.-L.; Song, H.-S. Entanglement between two Tavis–Cummings atoms with phase decoherence. *J. Mod. Opt.* **2009**, *56*, 496. [CrossRef]
52. Bashkirov, E.K.; Rusakova, M.S. Entanglement for two-atom Tavis–Cummings model with degenerate two-photon transitions in the presence of the Stark shift. *Optik* **2012**, *123*, 1694. [CrossRef]
53. Abdalla, M.S. Statistical properties of a transformed Tavis-Cummings model. *Phys. A* **1991**, *179*, 131. [CrossRef]
54. Chaichian, M.; Ellinas, D.; Kulish, P. Quantum algebra as the dynamical symmetry of the deformed Jaynes-Cummings model. *Phys. Rev. Lett.* **1990**, *65*, 980. [CrossRef]
55. De los Santos-Sanchez, O.; Recamier, J. The f-deformed Jaynes–Cummings model and its nonlinear coherent states. *J. Phys. B At. Mol. Opt. Phys.* **2012**, *45*, 015502. [CrossRef]
56. Dehghani, A.; Mojaveri, B.; Shirin, S.; Faseghandis, S.A. Parity Deformed Jaynes-Cummings Model: Robust Maximally Entangled States. *Sci. Rep.* **2016**, *6*, 38069. [CrossRef]
57. Friedrich, B.; Herschbach, D. Alignment and trapping of molecules in intense laser fields. *Phys. Rev. Lett.* **1995**, *74*, 4623. [CrossRef] [PubMed]
58. Eleuch, H.; Guérin, S.; Jauslin, H.R. Effects of an environment on a cavity-quantum-electrodynamics system controlled by bichromatic adiabatic passage. *Phys. Rev. A* **2012**, *85*, 013830. [CrossRef]
59. Wootters, W.K. Entanglement of formation and concurrence. *Quantum Inf. Comput.* **2001**, *1*, 27. [CrossRef]
60. Mandel, L.; Wolf, E. *Optical Coherent and Quantum Optics*; Cambridge University Press: Cambridge, UK, 1955.